Surface Dynamics of a DNA Loop Formation Using Surface Plasmon Resonance

By

Fuling Yang

A Thesis Submitted to the Graduate Faculty of
Auburn University
in Partial Fulfillment of the
Requirements of the Degree of
Master of Science

Auburn, Alabama
May 10, 2015

Keywords: thiolated DNA, methylene blue DNA, DNA loop,
surface characterization, surface plasmon resonance, free thiols

Approved by

Aleksandr Simonian, Chair, Professor of Material Engineering
Zhongyang Cheng, Professor of Material Engineering
Dong-Joo Kim, Professor of Material Engineering

Abstract

Electrochemical proximity assay (ECPA), was recently developed for direct protein quantitation as low as 10 fM. In this assay, the loop-like structure holds methylene blue (MB) in close proximity with the gold surface when the target is present, ensuring efficient electron transfer. However, for studying DNA binding dynamics on gold surfaces, investigations were carried out by immobilizing thiolated DNA onto the gold surface of the SPR sensor chip to form self-assembled monolayer. DNA loop oligonucleotides and MB-DNA sequences were alternately hybridized to the complementary strands to form a loop-like structure. Investigations on the formation of DNA loop like structure based on ECPA were carried out using surface plasmon resonance (SPR). SPR, is a well-established optical technique for studying mechanisms of DNA immobilization and interactions of DNA molecules with gold surfaces in real time. The result shows obvious refractive angle change (ΔRA) corresponding to the DNA hybridization of the whole system while there is no discernible signal observed upon elimination sequences (thiolated DNA or DNA loop) of DNA Loop based ECPA system. Furthermore, investigation on optimization of concentration and condition of SH-DNA in flow mode was carried out. Before thiolated DNA was self-assembled on the gold surface, it was treated with a reductant TCEP for cleaving the disulfide precursor. This leads to the release of free thiols and other sulphur derivatives. In order to study the effect of interference of free thiols, the SH-DNA after treatment was purified and compared with non-purified DNA. Further study was conducted to observe the effect of purified DNA on the sensitivity and enhancement of signals on DNA Loop based ECPA system. Mixture of different

ratios of free thiols (MCH) and purified SH-DNA was investigated for immobilization on gold surface. Through studying surface dynamics of DNA Loop based on ECPA system, we expect a significant improvement on sensitivity with ECPA- based biosensor.

Furthermore, effect of the presence of free thiols, produced by the presence of reductant often used to cleave disulfide precursors on SH-DNA self-assembly process, was investigated. We found that the SH-ssDNA binding on the gold surface was affected by the presence of these free thiols. With purification it was observed that purified SH-DNA led to surface hybridization enhancement in target binding signal by 39%. To study the presence of contaminants in non-purified and purified SH-DNA, the surfaces were characterized by UV-vis spectroscopic techniques. Different ratios of purified SH-DNA to free thiols demonstrated that the effect of binding intensities corresponding by ΔRA and the surface coverage. With this proof-of-concept study on the dynamics of the DNA loop model system, we anticipate the feasibility of this study in improving the speed and sensitivity of ECPA-based protein recognition.

Acknowledgements

First of all, I would like to convey my sincere and deepest appreciation for my mentor, Dr. Aleksandr Simonian, for his continuous support and guidance on my project and my graduate education as a whole. His continuous support and valuable suggestion play a significant role in this project. I will cherish these advice and inspiration he gave, not only in this project, but also in my life. I would also like to thank Dr. Zhongyang Cheng and Dong-joo Kim for their guidance and participation in my thesis committee. Also I would like to thanks to all teachers in I taken courses, who give me knowledge and inspiration in science and technology.

I would like to thanks my all colleagues in this project, specially, Dr. Mary Anitha Arugula, and Yuanyuan Zhang, who help tremendously and have illuminating discussions with me in this project. Also, I would like to thanks for Lang Zhou and Alina Chanysheva for assistance during I do experiments and contribute to more comfortable environment in our laboratory.

My friends lead to my life in auburn more colorful and happy. Thanks to my friends, Yuanyuan Zhang, Anqi Zhang, Xingxing Zhang, Yang Tong, Songtao Du, Cheng Chen, Yan Chen, Bethany Brooks for their willing assistance in my life and thus make life easier. Also, thanks to them for conducting me in dealing with various difficulties. Also, I need to thank all my friends I meet in auburn, Lulu Jiang, Yusheng Ding, Dan Zhang, Chen Liang, Yaqun Li, Lang Zhou, Honglong Wang, Zhizhi Sheng, Liangxi Li, Wenya Du, Jiahui Xv, Lin Zhang, Jiajia Hu, Yating Chai, Jinglie Zhou, Ennji Lee, Hyejin Park, MariAnne Sullivan, Steven Moore, Sadhwi Ravichandran, and Naved Siddiqui.

Most importantly, I want to express my deepest gratitude to my parents, my sister, and my brother for their love and encouragement in my every part of life, which give me power and motivation in my during my education life and throughout my whole life. Finally, I would special thanks to my fiancé, Dr. Jing Dai, who cherishes and loves me always, for emotional support and encouragement at every aspect of life and education.

Table of Contents

List of Tables

List of Figures

Chapter 1: Introduction

1.1 Motivation for research

During last three decades, there is momentous advance in the development of highly selective and sensitive sensing systems. They have many diverse applications for monitoring of various parameters in medicine, science, environment, and industry. Especially in health care and medical treatment, diagnostics is most critical steps in determining life and death of human. Two common methodologies in clinical and research laboratories are sandwich enzyme-linked immunosorbent assay (ELISA) and proximity ligation assay (PLA). However, ELISA is time-consuming, laborious and costly, and PLA is less sensitive and hard to read out. Thus, many scientists and engineers are more focused on developing more flexible, easy to use, and low cost but highly sensitive and accurate methods for medical diagnostics.

The electrochemical proximity assay (ECPA), a new developed assay for protein quantitation, is highly sensitive in detection of insulin concentrations (as low as 128fM), with the direct electrochemical readout. However, since this method is still in early stage of development, surface dynamics of ECPA on gold surface has not been explored. Surface plasmon resonance (SPR), an optical technique, is an ideal tool for characterizing surface binding properties. Also, Surface dynamics provides the information about their proper conformation, activities, and stability. Well known to be the ideal system to interrogate the surface interfaces, SPR has been widely used to characterize chemical structures and biomolecules on surfaces in a quantitative fashion and to test their proper orientation, conformation, activities and stability, etc. Here, we show SPR as a much universal

detection technique capable of monitoring surface hybridization and real-time monitoring of its events. In this study, we systematically investigated the self-assembly of thiol terminated single stranded DNA (SH- DNA) on gold for DNA immobilization on gold surfaces.

1.2 Overview

The aim of this project is to develop a new readout mechanism for ECPA, and thoroughly characterizes surface dynamics of ECPA at all stages, providing the new knowledge for optimization and expansion. In chapter 1, I discuss the motivation of this study and overview the organization of this thesis. The motivation introduces the significance of this project and its advantages. Also, overview gives reader organization of this thesis. Chapter 2 discusses fundamental concept of sensors including DNA sensor and optical sensor. This section focuses on the trend of DNA biosensor development through discussing the principle and comparing its advantages and disadvantages. In addition, the third part of this chapter gives literature review of the history, principle of surface plasmon resonance, and the devices used in the SPR techniques. The last section of chapter 2 introduces various methods of immobilization for DNA. The first section of chapter 3 discusses the objectives of the thesis and materials and methods for preparation before using SPR instrument, including the preparation of gold sensor, filtration matrix, simple concept of SPR set up, and details on the parameter set in software. The operation procedures for each experiment are included in the last section of chapter 3. Several figures are present to provide clear illustrations of operation procedures. Chapter 4 presents the results and discussion of this project. Chapter 5 summarizes the conclusions and the future work.

Chapter2: Literature review

2.1 Introduction to sensor

In nature, the term "sensor" can be applied to every living organism. For human, the sense organs, such as, eye, ear, nose and tongue and so on, contribute to exploring wonderful life through seeing, hearing, smelling, and tasting. With the development of technology and science, human obtain inspiration of sense organs and thus create artificial system called sensors that have similar functions. Therefore, we can understand the definition of sensor in Merriam-Webster: *a device that responds to a physical stimulus (as heat, light, sound, pressure, magnetism, or a particular motion) and transmits a resulting impulse (as for measurement or operating a control)*[1].

In general, a sensor consists of three parts: detection element, transducer and signal processor (**Figure2-1**). Detection element is responsible for detecting sample or target. The response from detection element is converted to a signal by transducer, and signal processor processes signal human can observed. Usually, sensors can be classified into three types: (a) physical sensor measures the physical properties of analytes, such as the length, mass, temperature and else; (b) chemical sensor for monitoring chemical elements of one or multiple chemical substances, determining those chemical substances' quantities and qualities[2]; (c) biosensor, a branch of chemical sensors in consideration sometimes, can be used for measuring biological samples[3]. The main difference between biosensor and chemical sensor is biological component involved.

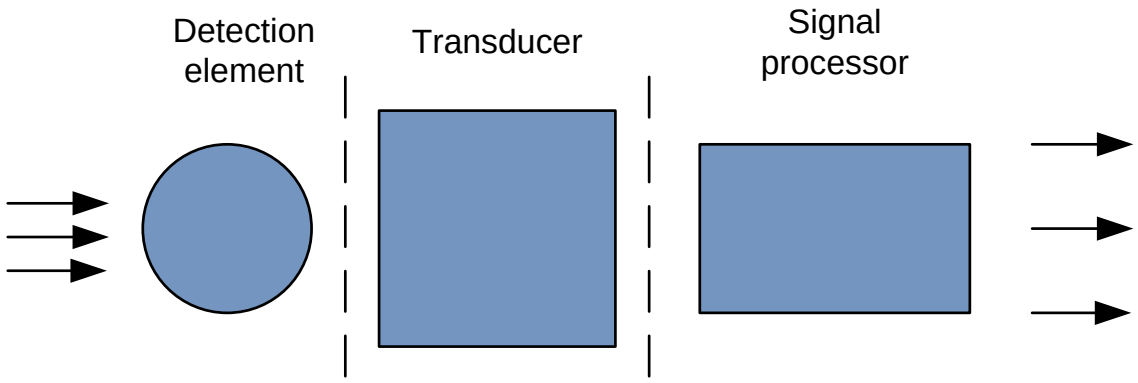

Figure2-1: A schematic layout of a biosensor. A biosensor includes detection element, transducer, and signal processor.

Image modified from Eggins, B.R., Chemical sensors and biosensors. Analytical techniques in the sciences. 2002

2.2 DNA detection systems

Biosensor is an analytical device, which usually contains following parts: one or more bioreceptors (enzyme, antibodies, nucleic acids, microorganism, chemo receptors, tissue, and organelles), one kind of transducers (electrochemical, optical, piezoelectric, calorimetric), and a signal processor[4]. DNA biosensor uses DNA as a bioreceptor combined with various transducers[5]. DNA biosensor is one of the most popular biosensors. DNA material can be widely used and it is cheap. Moreover, its interaction principle can be well-understood. DNA can form secondary and tertiary structure, showing different properties and different functions for the diagnostics and biosensor study research.

2.2.1 DNA structure and its interaction

Deoxyribonucleic acid (DNA) is a molecule that encodes genes that play an important role in the all living organism and virus. From the **Figure 2-2**, DNA is composed of phosphate esters of a five-carbon sugar and a nitrogenous base[6]. In DNA, there are four nucleotide bases: adenine (A),

guanine (G), cytosine (C), and thymine (T). It can bind together by hydrogen bonds between complementary base pairs and thus hybridizes to form a stable double helix. The principle of complementary base-pairing is: adenine is complementary with thymine by two hydrogen bonds (A-T); guanine is complementary with cytosine by three hydrogen bonds (G-C)[7]. DNA biosensor is based on the DNA hybridization.

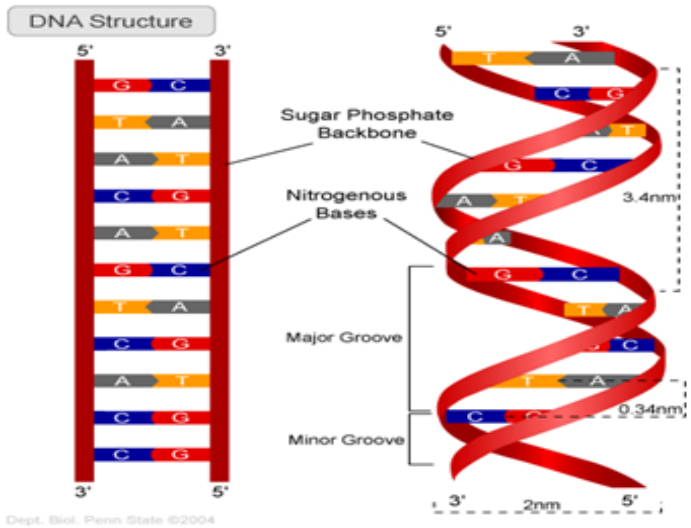

Figure 2-2: The structure of DNA. In DNA, there are four nucleotide bases: adenine (A), guanine (G), cytosine (C), and thymine (T).

https://sites.google.com/site/imlovingmygenes/dna-structure

2.2.2 Transduction mechanisms in DNA biosensor

Transducing systems are divided into four types: thermal, electrochemical, optical, and piezoelectric. The following discussion will focus on last three transduction mechanisms[8].

2.2.2.1 Electrochemical

In the case of an electrochemical sensor, a single stranded DNA (ssDNA) was immobilized onto electrode surface[9]. Hybridization of immobilized ssDNA with complementary ssDNA with dye

label, produces the changes in electrical parameters such as current, voltage, conductance, impedance, capacitance and else. Electrochemical sensors can be subdivided into three categories: (a) amperometric/voltammetric sensor, (b) potentiometric, and (c) conductometric.

Amperometric/voltammetric sensor measures current from oxidation or reduction that obey Faraday's law and law of mass transport[10]. In the case of voltammetry, most common analysis mode is linear sweep voltammetry (LSV) and cyclic voltammetry (CV)[11]. In two analysis modes, the potential is swept linearly with time and the current response is measured continuously by electron transfer. The significant difference between two modes is that, direction of the potential scan is reversed at the end of the first scan and the potential range can scan several cycles in CV, whereas the scan is only one direction. Amperometry is a similar technique as voltammetry[12]. The key difference is that, amperometry is the measurement of a constant or stepped potential whereas voltammetry is the measurement of controlled range of potential. Amperometry usually has two operation modes: batch mode and flow mode. Batch mode yields steps in signal whereas the flow mode provides peaks in signal.

Potentiometric sensor measures the interfacial potential by charge distribution between interface of electrode surface and solution[2]. The cell consists of both an indicator and reference electrode, sometimes with membrane, which means only certain ions can pass through it. There is no current flows during measurement of the solution potential to keep its composition unchanged[13]. The most common type of reference electrodes is Ag/AgCl and Hg/ Hg_2Cl_2[14].

Conductometry is a measurement of electrical conductance in an electrolyte solution by means of a conductometer [15]. The instrument of conductance consists of an alternating current source, conductivity cells, and electrodes. When electrical potential is applied across electrode, ions begin to accumulate near the electrode and thus transfer of change through the interface. The electric

conductance in accordance with ohms law, which states the strength of current transverse, conductor is proportional to potential difference and inversely to resistance[16]. Electric conductivity of an electrolyte solution depends on, type of ions (cations, anions, slightly or doubly charge) concentration of ions, temperature, mobility of ions, and else.

2.2.2.2 Piezoelectric

Piezoelectric sensor measures electric charge generated from the changes in mechanical stress when DNA sequence immobilization on the surface of a piezoelectric solid material.[17] The most common piezoelectric solid material is quartz crystal[18]. A DNA sequence containing several hundred base pairs, which have enough high molecular weight, immobilizes on the surface of piezoelectric quartz crystal. With hybridization of another complementary DNA-chain, the fundamental resonance frequency shifts along with the mass change in surface due to hybridization of complementary counterparts. This is the famous quartz crystal microbalance theory[19]. Comparing with non-complimentary DNA immobilization on surface of quartz crystal, hybridization with complementary DNA-chain contributes to 100 Hz frequency increase on modified piezoelectric crystal surface.

2.2.2.3 Optical

In last thirty years, optical biosensors have a revolutionary development of DNA detection[14]. The most attractive advantage of optical biosensors is direct label-free sensing as signals are only related to molecular mass of DNA[20]. These sensors are highly sensitive as low as 10^{12}molecules/cm^2, which also provide real-time and non-destructive analysis[21]. Most optical biosensor is based on the spectroscopic techniques such as measurement of absorption, reflection, scattering, or fluorescence.

For the case of absorbance, optical sensors are used to detect light intensity that correlate to concentration of analytes, according to Lambert-beer Law[22], such as Fourier transform infrared spectroscopy[23] and ultraviolet-visible spectroscopy[24]. Fluorescence is the radiative deexcitation of a molecule after absorption of a photon[25]. These sensors provide information about the excited energy state and relaxation dynamics. Scattering light is divided into two major types[26]: (1) elastic scattering refers to photon energies of the scattered photons that leave the molecule in the same state, such as Rayleigh scattering; (2) inelastic scattering leaves the molecule in a different quantum state, and thus changing in vibration and rotation of energy of a molecule.

Reflectance sensors should have conditions of total internal reflection, thus creating the evanescent field[27]. In the total internal reflection condition, the angle of incidence is increased beyond the critical value, incident light can no longer refract into interface according to Snell's law[28]. Usually, for air-water, the critical angle is 43.75°[2]. However, the total internal reflection condition does not mean that there is no energy loss. A fraction of the radiation extends a short distance from the guiding region into the medium that has lower refractive index. The reflected beam with the incident light can form the standing electromagnetic wave at interface, which can penetrate the rare medium, called evanescent field[29]. One of most common methods in DNA detection is SPR. Following section will discuss SPR in detail.

2.3 SPR optical sensor

In 1900's, Wood first observed a phenomenon ''anomalous'' dark and light bands in the reflected light by shining polarized light on a mirror with a diffraction grating on its surface[30].Since then, the reason of such phenomenon in the vacuum by electron loss spectroscopy has been intensively studied. In 1907, Lord Rayleigh had an initial physical interpretation of such phenomenon[31]. In 1941, U. Fano first time demonstrated the existence of electromagnetic surface waves on a

metal/dielectric interface by fast electron passing through metal foils[32], but a completed explanation the phenomenon was impossible until 1957. Ritchie assigned the phenomenon that the energy loss of the electrons to the excitation of surface plasma waves[33]. Two years later, Powell and Swan confirmed the phenomenon of Ritched through energy loss in Aluminum[34]. Kretschmann[35] and Otto[36] at the same time reported the excitation of surface plasmon.

After that, Liedberg and his lab mates applied the SPR for gas detection in 1983[37], which is the first application of SPR. Seven years later, application of SPR promoted the booming of interaction of receptor-ligand. In 1990, Pharmacia Biosensor AB released the first commercial SPR product--Biacore instrument[38]. Since then, a few scientists used SPR-based biosensor as an analytical tool for their projects. Their success confirmed the ability of the SPR-based biosensors in the receptor-ligand interaction.

2.3.1 Principle of SPR

Surface plasmon resonance, is an optical phenomenon, measuring the refractive index of a layer between solution and a very thin metal coated prism[39]. When a small beam of incident light passes through back side of prism at certain defined angle, the energy interacts delocalized electron in the metal film (plasmon) and thus reduces the intensity of reflected light. At certain condition, depending on the refractive index of the absorbate, surface plasmon on the metal film can be excited by photons, and thus transforms a photon into surface plasmon[38]. **Figure 2-3** is the most common geometrical setup.

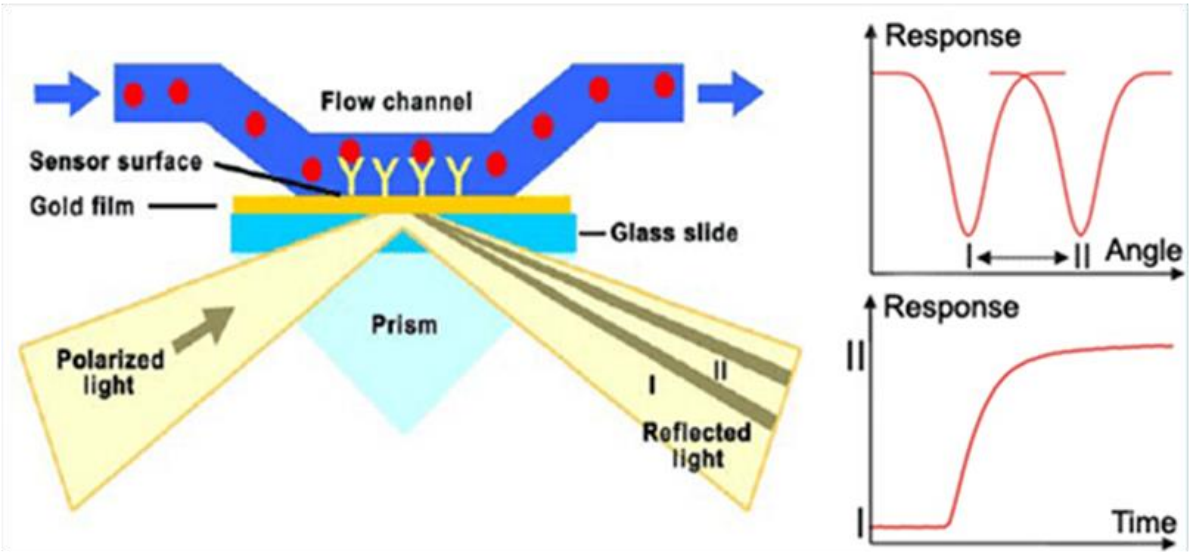

Figure 2-3: The most common geometrical setup of SPR

http://web.bf.uni-lj.si/bi/sprcenterTechnology.html

From this geometrical setup of SPR, the incident light is usually located on glass side of the metallic film because surface plasmon cannot be excited by photon as surface being hit. Actually, an evanescent light field can be induced by photon into metallic film and thus no photons can pass through this field in normal condition. Only some photons in certain angle are able to take place through this field, thereby, it causes surface plasmon on the adsorbate side of metallic film. One photon disappears and produces a dip in reflected light at certain angle as a plasmon is excited. Also, this angle is dependent on the refractive index in the absorbate layer. The extent of binding between the solution-phase absorbate and the immobilized absorbate is easily observed and quantified by monitoring this refractive angle change[40]. An advantage of SPR is high sensitivity without any fluorescent or other labeling of the absorbate.

2.3.2 Devices to induce SPR instrument

Devices of a surface plasmon resonance instrument are mainly divided into three systems (**Figure 2-4**): Optical system, sensor system, and detection system. Optical system is the most significant detection system, which includes the light source and the optical path; the sensor system that can transform the sensitive information by refractive index changes of the thin film to the detection system, based on the principles mentioned above; detection system detects the intensity of the reflected light and record the resonance absorption peak for further analysis[41].

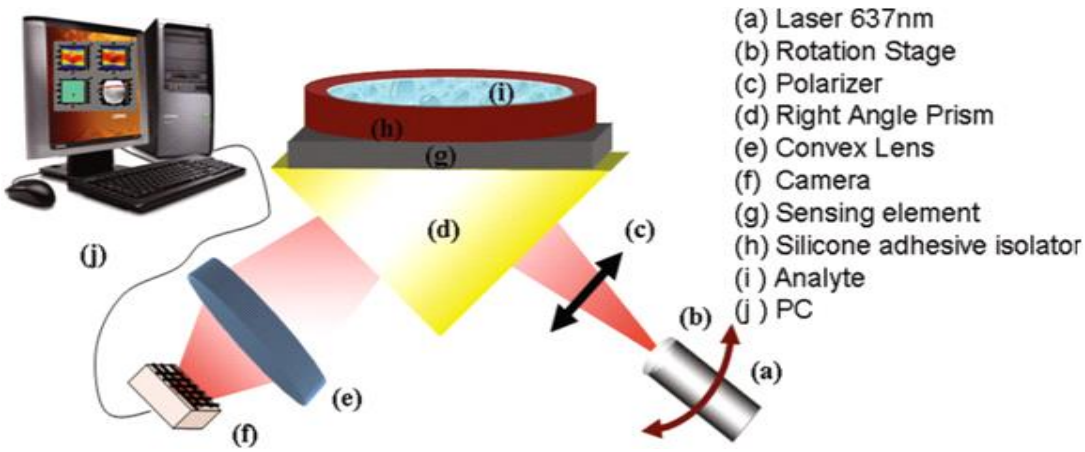

Fig 2-4: The devices for a Surface Plasmon Resonance instrument

Image modified from Karabchevsky A, Karabchevsky S, Abdulhalim I, Nanoprecision algorithm for surface plasmon resonance determination from images with low contrast for improved sensor resolution. J. Nanophoton, 2011

2.2.2.1 Optical system

The optical system for SPR includes light source and optical path mechanism. The light source should be monochromatic and p-polarized (polarized in the plane of the surface) to obtain a sharp dip, which is usually in a high efficiency near-infrared light. The light that is not p-polarized will

not contribute to the SPR and will increase the background intensity of the reflected light[39]. Optical path mechanism is based on prism couplers, the most commonly used materials are optical glasses. The material of the glass is chosen based on the analytes refractive index range to be covered by the sensor. Some scientist tried to plastic prism to substitute the glass one, leading to disposable cost-effective sensing element. For excitation of SPR, the grating couplers are usually produced by the holographic technique in the interference of two laser beams[39].

2.2.2.2 Sensor system

Various metals have been examined for utilization in SPR sensor. Gold and silver are most commonly active metals used in SPR sensor[42]. Compared to gold, silver coated in the sensor surface is more sensitive, but the long-term stability of silver is still very poor. The thin layer of SPR active sensor is mainly treated by vacuum evaporation and sputtering. Additional layer from dielectrics is usually made by MgF_2, Ta_2O_5, TiO_2, SiO_2, and used to optimize the performance of waveguide- based SPR[43]. In the chemical SPR sensor, the transducing layers are often formed from polymer, such as polysioxanes, teflon, polysiloxanes, et al. Methods including spin coating and dip coating techniques can produce thin optically homogenous layers of the polymers. Based on structure of the optical system, the current SPR sensor system can be divided into four structural types: optical prism couplers, grating couplers, optical waveguides, and optical fiber.

2.2.2.3 Detection system

The SPR sensor detection methods can be classified into the four types. First, monochromatic incident light passes through prism, changes the incidence angle, then detects the changes of the normalized intensity of the reflected light with the change of the incidence angle, and finally records the incidence angle. Second, the incidence angle is fixed, and the reflectivity of the wavelength being changed, then the resonant wavelength is observed. Third, both the wavelength

and the angle of the incident light are fixed, the phase difference of the incident light and reflected light is recorded. Fourth, when the wavelength and the angle of incident light are fixed, the changes of the refractive index are analyzed by measuring the reflected light intensity. Except for impractical method of last method, the first two types of methods are commonly used in application and the third method has the maximum sensitivity, but it requires a series of high frequency circuits[44].

2.4 DNA immobilization methods

Immobilization is significant for surface chemistry, which is able to stop the reaction rapidly by removing the analytes from the reaction solution. There are a lot of advantages of immobilization: enhanced stability, predictable decay rates, elimination of reagent preparation, low cost, and higher purity product. In general, we have four principle methods[45] for immobilization of DNA: (a) Physical adsorption: it simplest method and involves reversible surface interaction between DNA and support material. The forces involved are mostly electrostatic, such as van der Waals force, ionic and hydrogen bonding interaction. Even though these forces are too weak, it is sufficiently large in number to enable reasonable binding. (b) Entrapment: this immobilization contributes to DNA that can be free in solution, but restricted in movement by the lattice structure of a gel. (c) Covalent binding mode: it is one of the most intensively studied immobilization techniques, it is the formation of covalent bond between the DNA and support matrix. (d) Encapsulation: it is similar to entrapment for DNA that can be free in solution, but this type is restricted in space. **Figure 2-5** is the overview of these four immobilization methods.

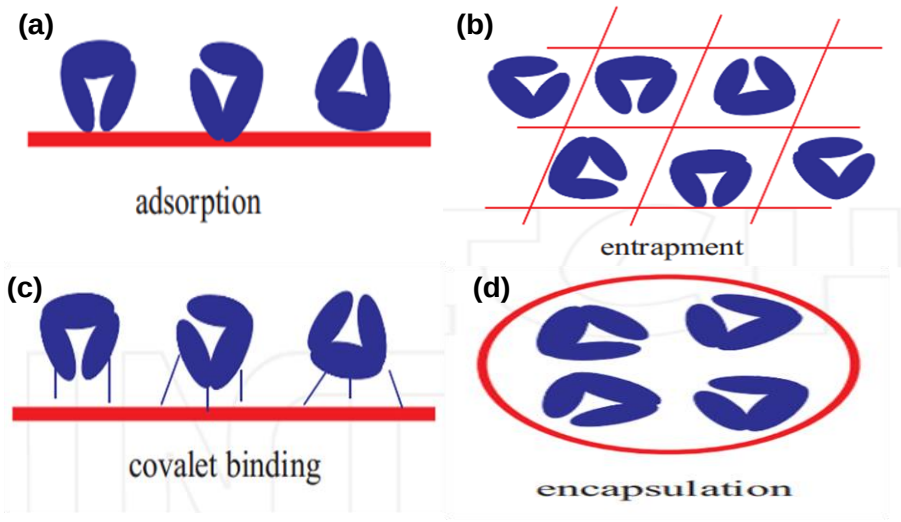

Figure 2-5: Illustrations of four methods of immobilization: (a) adsorption; (b) entrapment (c) covalent binding method (d) encapsulation

Image modified from Xiuyun Wang and Shunichi Uchiyama, State of the Art in Biosensors-General Aspects, 2013

Chapter 3: Materials and methods

3.1 Objectives

The objective of this study is to develop a new mechanism for electrochemical proximity assay (ECPA) shown in following:

- Develop a new readout mechanism for ECPA, surface plasmon resonance (SPR).
- Monitor stepwise assembly of SH DNA, DNA loop and MB DNA and timing of DNA hybridization.
- Investigate effect of free thiols of DNA assembly on gold surfaces.
- Study the difference between Purified and Non-purified thiolated DNA.
- Investigate the increase of sensitivity of target binding**.**

3.2 Materials and Instrumentation

3.2.1 Reagents and materials

The following reagents were used as received: 4-(2-hydroxyethyl)-1-piperazineethanesulfonic acid (HEPES) (99.5%) was purchased from Alfa Aesar. Tris-(2-carboxyethyl) phosphine hydrochloride (TCEP), 6-Mercapto-1-hexanol (MCH, ≥97%), ammonium hydroxide (volumetric, stand 5.0N solution in water) and Tris(hydroxymethyl) amino methane (ACS reagent, 99.8%) was purchased from Sigma-Aldrich (St. Louis, MO). Methylene blue-conjugated DNA - 27 - (MB-DNA) was purchased from Biosearch Technologies (Novato, CA), purified by RPHPLC. Thiolated DNA (SH DNA) and DNA loop oligonucleotides were purchased from Integrated DNA Technologies (IDT, Coralville, Iowa), with purification of HPLC. Methylene blue-conjugated

DNA was obtained from Biosearch Technologies (Novato, CA), with purity by RP-HPLC. Hydrogen peroxide (ACS, 30%) and Ethylenediaminetetraacetic acid (EDTA, ≥99%) was purchased from Fisher Scientific (Fair Lawn, NJ). Sodium perchlorate anhydrous (ACS, 98.0-102.0%) and Alcohol anhydrous (ACS, ≥99%) were purchased from VWR International (LLC Radnor, PA). DNA wash buffer and oligo binding buffer and Zymo-Spin Column were purchased from Zymo Research (Irvine, CA). Desalting column (Glen Gel-Pak 1.0) was obtained from Glen Research (Stering, VA).

Name	Sequence
Thio-DNA	5ThioMC6-D/GCA TGG TAT TTT TCG TTC GTT AGG GTT CAA ATC CGC G
DNA Loop	TAG GAA AAG GAG GAG GGT GGC CCA CTT AAA CCT CAA TCC ACC CAC TTA AAC CTC AAT CCA CGC GGA UUUGAA CCC UAA CG
MB-DNA	CCA CCC TCC TCC TTT TCC TAT CTC TCC CTC GTC ACC AUG C

Table 3-1: Sequences of ssDNA strands used in the ECPA experimental model are given

3.2.3 Instrumentation

3.2.3.1Surface Plasmon resonance

The **Figure 3-1** is the SPR Bionavis 210. SPR instrument used in the measurements was a BioNavis SPR Navi 200-L (Tampere, Finland), equipped with 785 nm and 670 nm light sources. The instrument includes built-in degasser, automated valves and syringe pumps. Key features include true goniometric SPR with wide angular scan range (38°-78°), customizable flow cell and a flexible sensor slide system to easy drop in placement. The liquid handling in the experiments was performed using the built-in peristaltic pump and 12-port chromatography injector, and the

flow cell has 1µL inner volume. All measurements were performed at 25 °C. SPR gold sensor slides were obtained from BioNavis (Tampere, Finland) and used immediately after cleaning with a hydrogen peroxide-ammonia-water solution according to the protocol suggested by the manufacturer. The SPR Bionavis 210 instrument was controlled by a SPR Navi Control. All experiment was performed at room temperature. After calibration with air, buffer was allowed to flow through at flow rate of 30µL/min. Calibration with buffer was performed and custom angle range from 58° to 75° was set for further measurement. The angle resolution was 1/4 in a second with scan interval times around 16s. The SPR data were analyzed using the SPR Navi Data Viewer program. Conventional or "standard" SPR sensograms, monitoring purely the refractive index ns, are reported as Δθ values in unit of degree.

Figure 3-1: SPR Bionavis 210
http://www.bionavis.com/products/spr-navi-210a

3.2.3.2 UV-Vis Absorbance Spectroscopy

UV-vis measurements were conducted using Ultrospec 2100 pro, from GE Healthcare Life Science (Piscataway, NJ). SWIFT II software controls the instrument, which sets the parameters and collects the data. HEPES buffer was used as a blank. The absorbance values of all single stranded DNA were monitored at 200nm-320nm at room temperature.

3.2.3.3 Nanodrop spectrophotometer

All single stranded DNA concentrations were measured on Nanodrop 2000c, purchased from Thermo Fisher Scientific (Waltham, MA). 2µL of sample solution was used for measurement at room temperature. HEPES buffer was used as blank. This instrument can collect the spectra at a wavelength range from 190nm to 840nm.

3.3 Preparation for SPR instrument measurements

3.3.1 Preparation of sensors slides

3.3.1.1 Sensor slides

All SPR based experiments were performed on gold sensor slides. The sensor slides have three layers: glass substrate, adhesion layer, and plasmonic layer. The plasmonic layer is made of gold. The size of all sensor slides was 12×20mm for fitting the SPR Navi sensor holder. **Figure 3-2** shows a sensor slide used in the experiment and key element in the sensor slides.

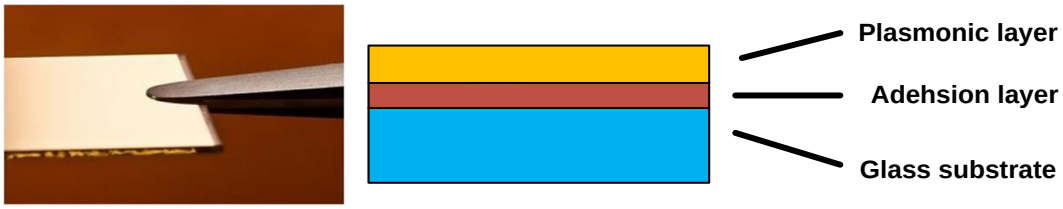

Figure 3-2: The sensor slide using in experiment and key element in sensor slide. http://www.bionavis com/ products/ consumables/

3.3.1.2 Procedure of sensor slide cleaning

The gold slides were initially cleaned in a boiling 1:1:5 solution of hydrogen peroxide-ammonia-water for 10 minutes. The slides were later washed carefully with plenty of water, and ethanol followed by drying with nitrogen. The cleaned slides were carefully placed on the slide holder provided by the manufacturer and inserted for the DNA detection. Prior to the immobilization of DNA, 1 µL of 200 µM thiolated-DNA was mixed with 2 µL of 10 mM TCEP in a 1.5 mL micro centrifuge tube. This tube was incubated in dark for 1 hr at room temperature (21°C) for reduction of disulphide bonds in the SH-ssDNA. The solution was then diluted to a total volume of 500µL or 1000µL in HEPES/$NaClO_4$ buffer (10 mM HEPES and 0.5 M $NaClO_4$, pH 7.0) to a final concentration of 1µM. Stock concentrations of MCH, DNA loop and MB DNA were prepared in HEPES buffer and diluted to 1mM MCH, 100nM DNA loop, 100 nM MB-DNA for analysis.

3.3.2 Setup for SPR monitor

Figure 3-3 shows layout of SPR monitor. Bionavis 210 connected peristaltic pump by tubing (length is 65cm; cross-section area radius is 1mm). Prior to staring experiment, tubing and flow cell are automatically washed by ethanol and deionized water. HEPES Buffer as baseline is introduced flow cell at 50 µl/min until single reaches to stable. Then, DNA sample is pumped into flow cell and it may take 15 min for full tubing. DNA sample is circulated within tubing until its signal becomes stable, then the pump is paused for several seconds and buffer is introduced to wash out unbinding DNA on gold surface. Repeat this procedure every time when changing another DNA sample.

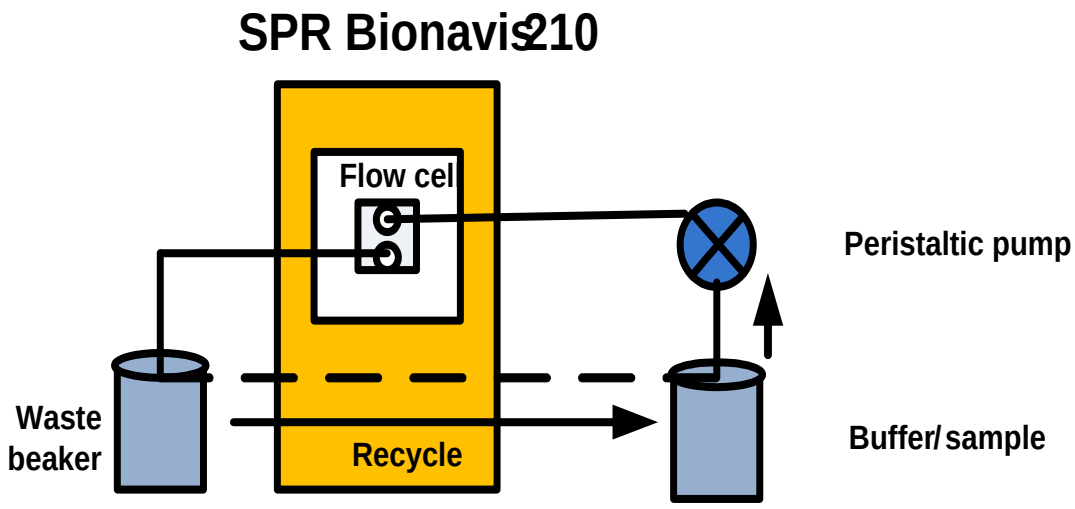

Figure 3-3: **The layout of SPR monitor. Bionavis 210 connected peristaltic pump by tubing (length is 65cm, cross-section area radius is 1mm).**

3.3.3 Parameters in software

The SPR Bionavis 210 instrument was controlled by a SPR Navi Control. The flow rate is 30µL/min. All experiments were performed at room temperature. Custom angle range was from 58° to 75°. The angle resolution is 1/4 in a second. The scan time was around 16s for custom angle range.

3.4. Treatment of thiolated DNA

All DNA solutions were prepared with HEPES buffer (HEPES: 10mM, sodium per chlorate anhydrous: 0.5 M, PH 7). HEPES buffer were stored in room temperature for 20 days. 1µL of 200µM thiolated DNA was mixed with 2µL of 10mM TECP for 1 hour in a 1.5 mL microcentrifuge tube. This mixture solution was incubated in dark for 1 hour. This solution was then diluted to a total volume of 500µL or 1000µL in HEPES buffer to a final concentration needed in this project.

3.5 Filtration of non-purified thiolated DNA

Two methods were used to purify thiolated DNA. A) This procedure is for preparing pure thiolated DNA. 5µL, 7.5µL, 15µL of 200µM thiolated DNA was mixed with 10µL, 15µL, 30µL of 10mM TCEP in 1.5mL microcentrifuge. These solutions were incubated in dark for 1hour. After 1hour, 35 µL, 12.5µL, 5µL of HEPES was added separately into three mixture solutions (2µM, 3µM, 6µM) for a minimum volume 50µL for purification system. 100µL oligo Binding Buffer was added into the three samples. Then 400µL ethanol (95-100%) was added and mixed briefly by pipetting and transferred those mixtures to Zymo-spin Column separately in three collection tubes. All samples were centrifuged at ≥10000×*g* for 30 seconds and the flow-through was discarded. Then 750µL DNA wash buffer was added to the column and centrifuged at ≥1000×g for 30 seconds and discarding the flow through. Three samples were then centrifuged at maximum speed for 1 minute. Sample was transferred to the column and 15µL of water was directly added to the column matrix. Then, these samples were centrifuged at ≥10000×g for 30 seconds to elute the thiolated DNA. Finally, 485µL HEPES was added to bring the final concentration of 2µM, 3µM, 6µM of purified SH-DNA. B) In other procedure using Gel-pak, the SH-DNA was mixed with TCEP for reduction of s-s linkage for 1h. The mixture was allowed to flow through 0.2 desalting column GEL-pak to separate free thiols and elution buffer was flowed through to drain pure SH-DNA. The DNA was later precipitated with ethanol and transferred to HEPES buffer for SPR measurements. All the eluting samples were later verified for DNA using UV-vis between 200-300nm wavelengths. Although this method was efficient, there was 20% loss of purified DNA during precipitation with ethanol.

3.5 Experimental procedures

3.5.1 Self- Assembly of thiolated DNA followed by DNA loop and MB DNA (ECPA system)

Prior to the installation of the sensor, the tubes were cleaned with ethanol and deionized water. The sensor surface for the DNA loop formation was prepared in the instrument by installing freshly cleaned sensor slide. HEPES buffer prepared earlier for sample preparation was allowed to flow through the flow cell at rate of 20µL /min until a stable baseline was observed. Next the sensor was functionalized with thiolated DNA by injecting 1µM SH- DNA until saturation of SPR signal was observed (10min). After washing with HEPES buffer to remove unbound DNA, the sensor was exposed to 1mM MCH to block the unreacted thiolated sites on the surface. In the next step, 0.1µM DNA loop oligonucleotide, with sequence complementary to half the SH- DNA was injected and allowed to bind until a stable SPR signal was observed. This step was followed by washing with buffer and injection of 0.1µM MB DNA, with a sequence complementary to the other half of DNA loop and SH- DNA and thus verifying the formation of loop like structure. In all the above cases, hybridization of the whole system was monitored for 10mins, followed by washing with HEPES buffer.

3.5.2 Procedures of control experiment in DNA Loop formation

All tubes were cleaned with ethanol and deionized water one time before experiments. HEPES buffer is as baseline for the whole experiment. The concentration of SH-DNA, DNA loop, and MB DNA are both 0.1µM in control experiment while concentration of MCH is 1mM. After HEPES signal is stability, the order of adding three types single strand DNA is SH-DNA, DNA loop, MB DNA. HEPES buffer was added to wash away unbind DNA sequence after each type DNA signal is stable. Three detections are required for control experiment. First experiment is to add four samples in following order: 1µM SH-DNA, 1mM MCH, 1µM DNA loop, 1µM MB DNA. Second

experiment is to add three samples in following order: 1mM MCH, 1µM DNA loop, 1µM MB DNA. Third experiment to add three samples in following order: 1µM SH-DNA, 1mM MCH, 1µM MB DNA. The flow rate is 30µL/min for three experiments.

3.5.3 Optimization of effect of increasing concentration of SH-ssDNA on gold sensor

SPR measurements were conducted to monitor the binding effect of different concentrations of thiolated DNA with increasing concentrations from 0.75µM to 6µMconsecutive injections.

3.5.4 Procedures of UV-vis detection for non-purified / purified SH-DNA, free thiols

HEPES buffer is used as blank throughout experiment. The concentrations of non-purified SH-DNA, purified SH-DNA, and free thiols were both 1.5µM. All sample measurements were done using quartz cuvette for UV-vis detection. Three experiments were performed in this section. First sample is non-purified SH-DNA, the thiolated DNA solution that has free thiols after treatment with TCEP. Second sample is free thiols, the solution that flowed through during filtration matrix. Third sample is purified SH-DNA, the solution that only has SH-DNA after filtration matrix.

3.5.5 Effect of purified / non-purified SH-ssDNA on gold sensor

The non-purified and purified SH-ssDNA samples of 2µM, 3µM, and 6µM concentrations were verified on SPR. After the signal of HEPES was stable, each concentration of non-purified SH-DNA and purified SH-DNA were injected into flow cell and increase in refractive angle was monitored. After each concentration of DNA sample reached stable value, HEPES buffer was injected for washing away loosely bound DNA.

3.5.6 Effect of sensitivity of DNA Loop formation using purified and non-purified SH-ss DNA

Measurements were conducted with purified and non-purified samples to test the sensitivity of binding of DNA loop and MB-DNA. The whole system binding was conducted using 2µM

purified DNA followed by 100nM DNA loop, 150nM MB-DNA. Similarly, another experiment was conducted with non-purified SH-DNA and was compared with purified SH-DNA. Here, the concentrations of DNA loop and MB DNA used in ECPA system were tested and the binding sensitivities were monitored. HEPES buffer was used as the baseline and for washing in between the DNA injections.

3.5.7 Effect in ratio of free thiols and SH-DNA for SPR detection

We investigated the effect of MCH treatment as free thiols on gold surface with two protocols: 1) with purified SH-DNA, pure MCH and non-purified SH-DNA and 2) co-immobilization of DNA and MCH at appropriate ratios with MCH. The percentage of purified SH-DNA was 100%, 75%, 50%, 25%, 0% while the percentage of free thiols (MCH) was 0%, 25%, 50%, 75%, and 100%. The concentration of purified SH-DNA and free thiols for each group are show in **Table 3-2**.

SH-DNA : free thiols	Concentration of Purified SH-DNA (µM)	Concentration of Free thiols (µM)
100:0	2	0
75:25	1.5	0.5
50:50	1	1
25:75	0.5	1.5
0:100	0	0

Table 3-2: The concentration of purified SH-DNA and free thiols.

Chapter 4: Results and Discussions

4.1 SPR monitoring response of stepwise of DNA Loop structure

In **Figure 4-1**, self-assembly of SH-DNA strands on the gold surface was demonstrated via thiol moiety at 5' terminus. The DNA loop based experimental model simulated the whole ECPA system. The cooperative hybridization of three DNA sequences is shown in experimental model: 3' terminus at thiolated DNA conjugated 5' terminus at DNA loop, and thus 3'terminus at DNA loop conjugated 5'terminius at MB DNA.

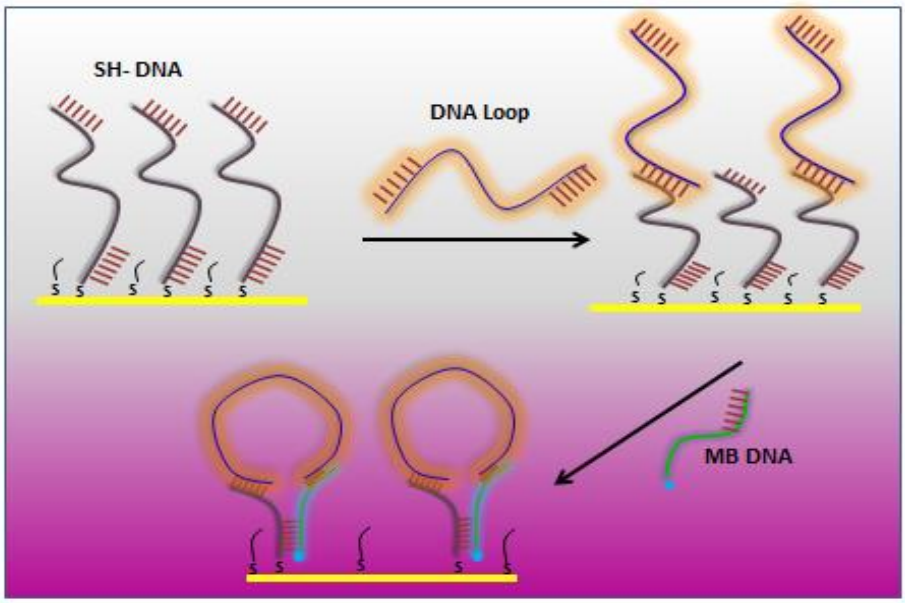

Figure 4-1: Schematics of DNA Loop formation

In **Figure 4-2**, each step of DNA sequence has an obvious refractive angle change in time period of ten minutes. The net refractive angle response of 1μM SH-DNA self-assembly on gold surface was 0.1°, 0.075° for 100nM DNA loop and 0.03° for 100nM MB-DNA. Change in refractive angle

was calculated by the change in initial refractive angle and stabilized angle in each corresponding DNA sequence after washing with buffer. This confirmed the high specificity of the ECPA system as demonstrated by surface plasmon. The hybridization sensogram are shown in **Fig 4-2** where the black curve showed the 785nm wavelength SPR sensogram. The sensogram showed clear evidence that MB-DNA and DNA loop oligonucleotides were alternately hybridized to the complementary strands (SH-DNA) immobilized on the sensor slide surface forming a loop.

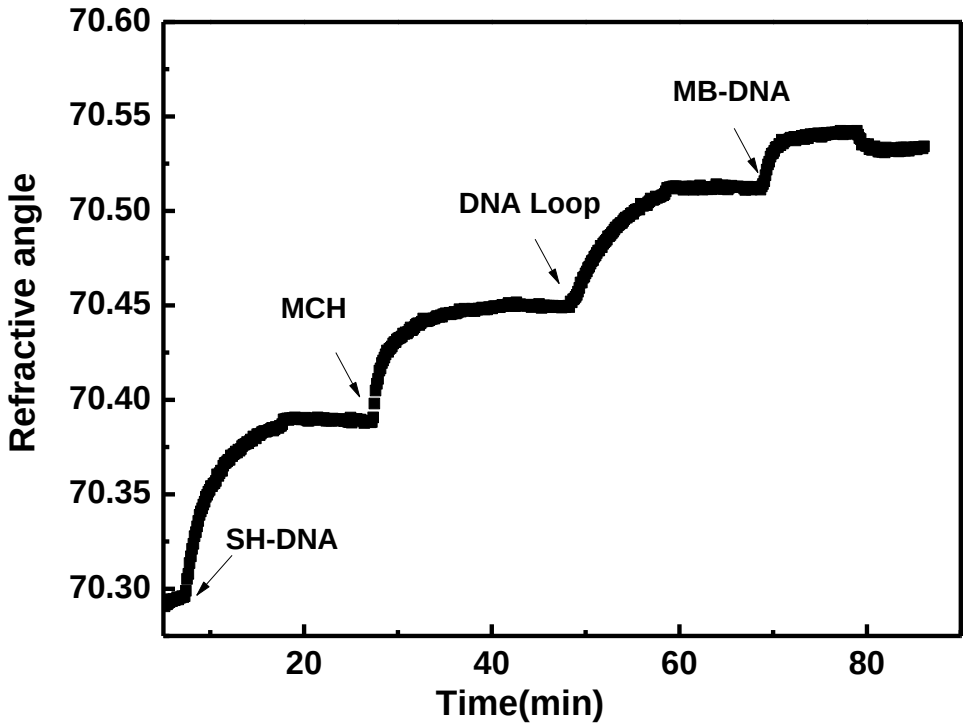

Figure 4-2: Stepwise of DNA Loop formation response on SPR monitor. DNA loop structure: 1µM SH-DNA, 100nM DNA loop, 100nM MB DNA at flow rate 30µL/min

4.2 Control experiment for dynamic DNA loop formation

The response curves in **Figure 4-3 A** shows a comparison between the SPR binding curves obtained with DNA loop formation and control experiments. The control experiments were used to determine the formation of loop when one of the DNA counter sequences were not injected.

Figure 4-3, shows that upon injection of SH-DNA (in black curve) there is an obvious signal observed after washing with HEPES buffer while red curve almost do not have signal change due to absence thiolated DNA covalent bond on gold surface. Since there is no SH-DNA bound, we observed that the red curve increased in signal upon injection of MCH and showed no further binding upon DNA loop and MB-DNA injections. This means only when thiolated DNA bond on gold surface, the DNA loop and MB-DNA can bind to their counterparts and demonstrate stable existence in DNA Loop structure sustaining the whole system. This is evident with black curve, that MB-DNA and DNA loop oligo were alternatively hybridized with SH-DNA. The green curve was obtained with SH-DNA immobilized and shows slightly higher signal than in black curve, however the signal remains stable after washing with HEPES, implicating the status of SH-DNA sequence bond in gold surface. It is likely that the DNA strands are either randomly laid down or upright in position, however, we assume that only upright strands could tightly bond on to the gold surface. After further binding MCH and washing, MB-DNA was directly injected. The green curve still have an obvious but small angle change comparing with same part in black curve, because even though there is no DNA loop in system complementary with MB-DNA, thiolated DNA still have one section complementary with MB-DNA with one terminus bond with another DNA sequence. Thus we observe no change in signal after washing with HEPES buffer, as these bonds are not very tightly bound. **Figure 4-3 B and Figure 4-3 C are** schematic of whole DNA loop based ECPA system and schematic of DNA loop based ECPA system without DNA loop sequence.

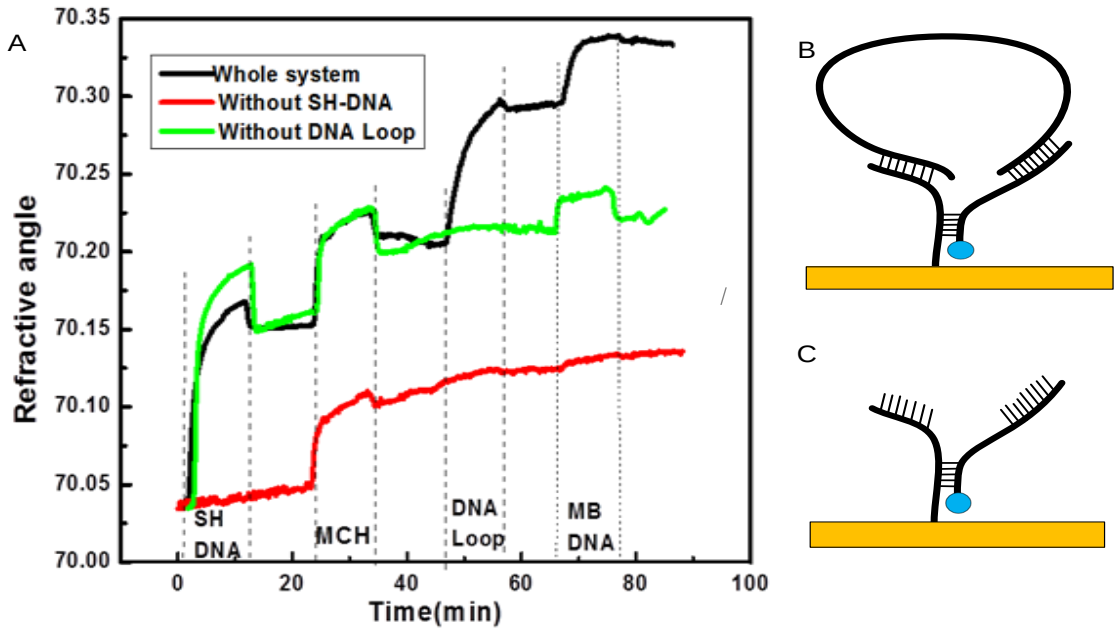

Figure 4-3: Control experiment of DNA loop based ECPA system. (a) Sensogram of SPR analysis three groups: whole DNA loop based ECPA system (Black line), DNA loop based ECPA system without DNA loop (green line) and DNA loop based ECPA system without SH-DNA (red line); (b) Schematic of whole DNA loop based ECPA system; (c) Schematic of DNA loop based ECPA system without DNA loop sequence.

Figure 4-4 shows bar graph in each group in control experiment, presenting the comparison of each group directly. In no DNA loop group, refractive angle change is 0.1° while the refractive angle is 0.47° in whole system, even though the refractive angle is almost same in the SH-DNA part of each group. That means DNA Loop in system can sustain the complementary MB-DNA and thus determine MB-DNA stable existence in DNA Loop system. In the no SH-DNA group, the refractive angle change of DNA loop and MB-DNA are 0.07° and 0.09°, while refractive angle change of these two DNA sequence is 0.9° and 0.47°, even though the same amount of DNA loop and MB-DNA are in the each group. It demonstrates that SH-DNA pay an importance role for holding whole system via thiol-gold covalent bond in gold surface.

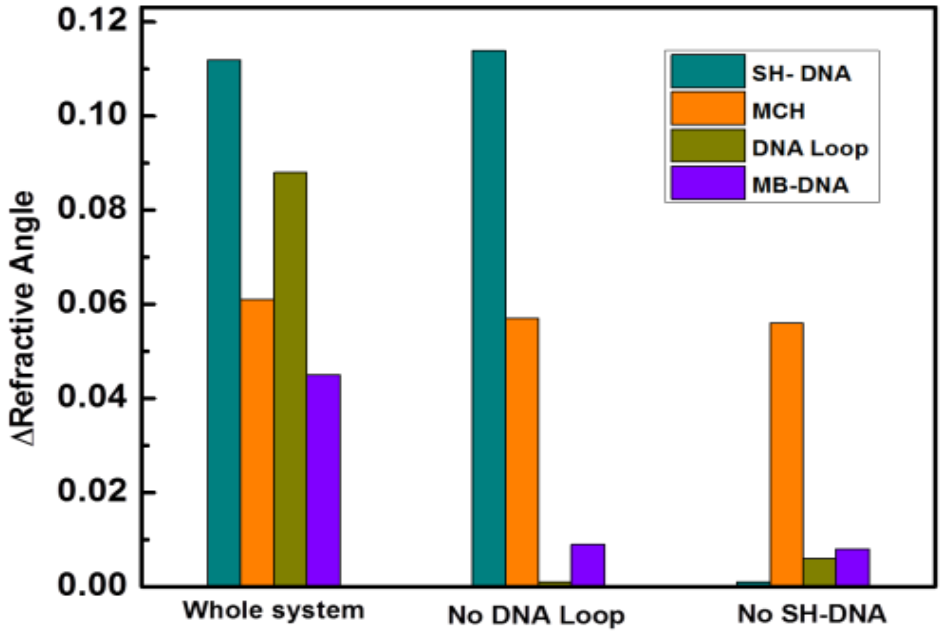

Figure 4-4: Bar graph of three group in control experiment. Green graph shows the refractive angle change of SH-DNA. Orange graph shows refractive angle change of MCH. Brown graph represents the refractive angle change of DNA loop. Blue graph shows refractive angle change of MB-DNA

4.2 Effect of concentration variation on binding

Increasing concentrations of SH-ssDNA after TCEP treatment was allowed to flow through and immobilized on the gold surface. Initially 0.75µM SH-DNA was injected and with increased concentrations we expected to observe increasing SPR signal before reaching saturation. However, with the initial and lower concentration there was a spontaneous binding of the thiol structures reaching saturated and stable signal within 10mins. Further injections did not give discernible increase in SPR signal. We therefore investigated the structure and coverage of the DNA film on the surface. It is known that high purity DNA is necessarily required to obtain meaning results in biosensor and biotechnology applications. From literature, it was found that the reductant treated

DNA to break the disulphide bond contains sulphur and free thiol contaminates due to the presence of excess of TCEP derivatives[46]. TCEP may interfere with the thiol immobilization and is reported to react with malemides under certain conditions. Moreover, TCEP treatment of disulphide DNA cleaves the disulphide linkage to remove free thiol groups SH-$(CH_2)_6$ and must be separated from the oligomers before they are attached to the gold surfaces.

4.3 UV-vis analysis of non-purified/purified SH-DNA and free thiols

For surface modification applications, it is necessary to investigate on the TCEP residuals and the binding thresholds that may interfere with SH-ssDNA assembly onto the gold surface. Upon Gel filtration with GEL-pak 0.2 desalting column, the eluting and purified DNA was measured. In **Figure 4-5**, UV-vis results show that the non-purified SH-DNA (green curve) show peaks at 260nm and 210nm, indicating the presence of DNA sequence and thiols. We also observed that the elute flow-through in filtration matrix, showed only one high absorbance peak around in 230 nm, which indicates the presence of free thiol derivatives (red curve). Interestingly we did not observe peak for DNA at 260nm which we have expected. The purified SH- DNA (black curve), showed similar peak at 260nm and 210nm, indicting the presence of DNA. However, the peak in 260nm was slightly lower in intensity compared to the peak of non-purified SH-DNA. We observed that gel filtration although, can show the separation of free thiols from SH- DNA unfortunately, and may not be 100% efficient procedure. Therefore, to avoid the DNA lost and achieve purified SH-DNA in HEPES buffer for direct usage in SPR measurements, we employed ZYMO spin columns for purification.

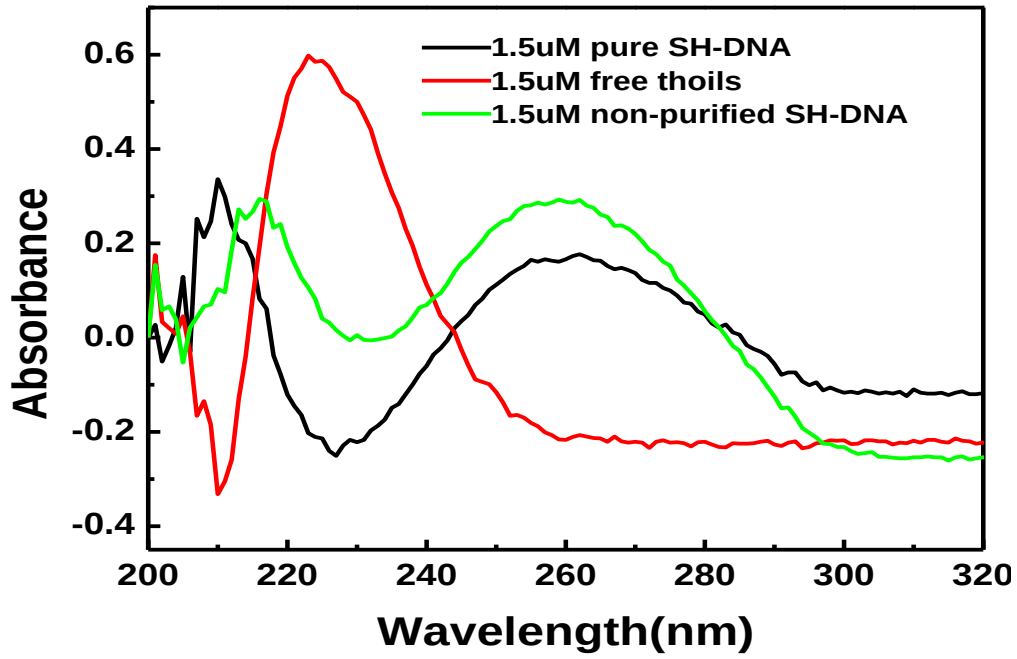

Figure 4-5: Analysis of UV-vis for purified SH-DNA (black), free thiols (red), non-purified SH-DNA (green)

After treatment with TCEP in dark for one hour, non-purified SH-DNA had pure SH-DNA in TE buffer. With filtration desalting column, flow-through was TE buffer and the remained in microcentrifuge tube was pure SH-DNA. From **Figure 4-6**, black curve is the pure SH-DNA in TE buffer showed peak in 260nm and 210nm, which means have DNA sequence and thiol group. Blue and green curve were two solutions flowing through by Zymo DNA concentrator, and thus they did not have peak around in 260 nm, which is SH-DNA concentrated in the column. For the red curve, the peak in 260nm and 210nm appeared again, that mean have SH-DNA.

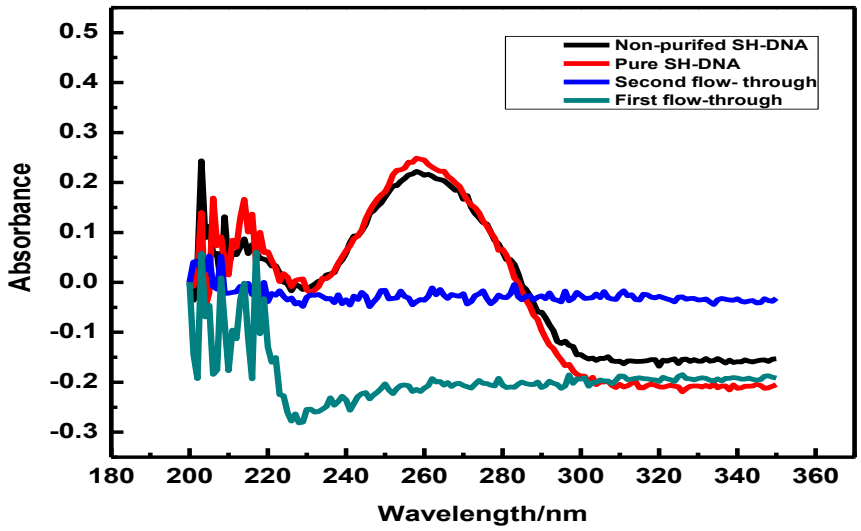

Figure 4-6: Analysis of UV-vis for pure SH-DNA in HEPES buffer(red), pure SH-DNA in TE buffer (black), First flow-through (green), Second flow-through (Blue) .

4.4 Effect of purified/ non-purified SH-DNA on gold surfaces

In **Figure 4-7A**, data show the comparison of pure SH-DNA and non-purified SH-DNA refractive angle change for 2µM, 3µM and 6µM concentrations. Although UV-vis results indicate the presence of free thiols it was not fully identified by SPR previously. Our investigation however observed that the purified SH-DNA binding onto the gold surface is much higher than non-purified SH-DNA within same concentrations. With several repeated experiments we obtained similar higher intensity of SPR signals for purified DNA. This leads to the conclusion that the presence of free thiols and reductant derivatives (sulphur contaminants) compete with SH-ssDNA binding onto the gold surface and thus significantly contribute to the lower binding of SH-DNA oligomer evident from low refractive angle change in non-purified samples. It is should be noted that from **Figure 4-7B** and **Figure 4-7C**, non-purified SH-DNA has free thiols $(SH\text{-}CH_2)_6$ concentration approximately close to SH-DNA after the s-s bond cleavage, since TCEP cleaves each DNA

oligomer. This can be estimated to be sufficient to affect the self-assembly of pure SH-ssDNA. Contrary, with purified samples the increase in SPR signal is attributed due to less or no competed free thiols groups and allowed for denser and thicker binding and of the SH-DNA. In literature XPS and TOF-SIMS analysis were performed to confirm that the presence of DTT concentrations as low as 0.001µM could affect the self-assembly of SH-DNA and surface composition of DNA films [47, 48].

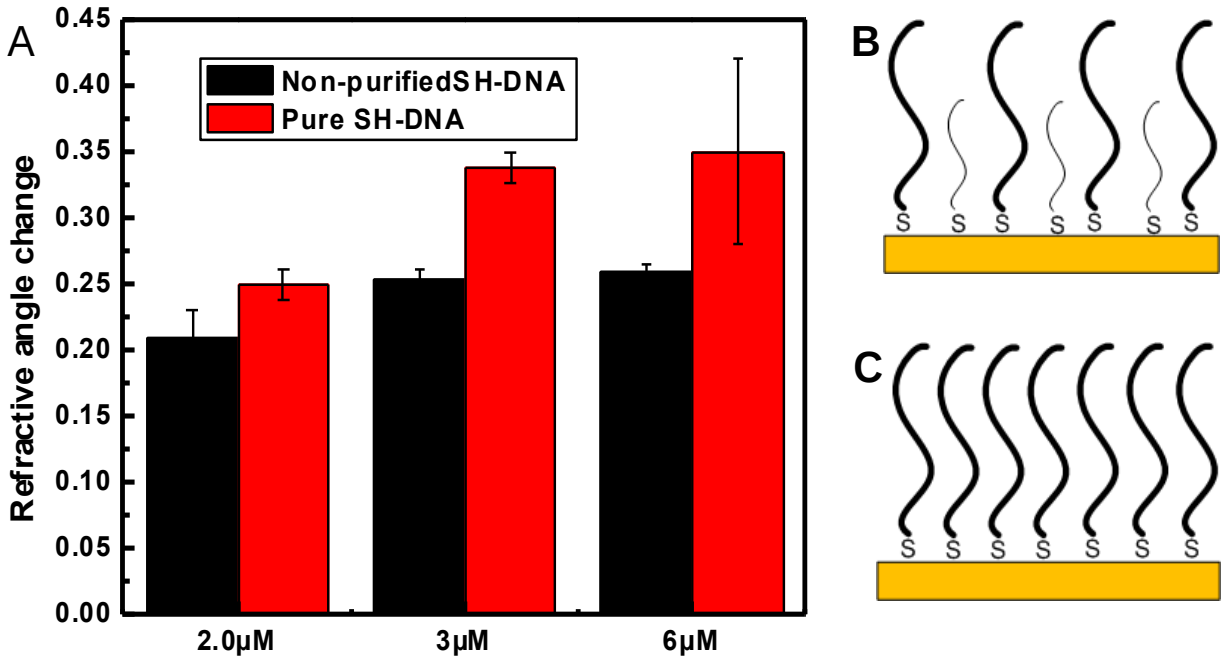

Figure 4-7: Comparison of pure SH-DNA and non-purified SH-DNA. (A) Bar graph of refractive angle change of purified SH-DNA (red) and non-purified SH-DNA (black). (B) Schematic of non-purified SH-DNA (C) Schematic of purified SH-DNA.

4.5 DNA loop formation sensitivity measurements with purified/non-purified DNA

In **Figure 4-8A**, the time of SH-DNA immobilized fully on gold surface was approximately 320 minutes. Comparison of 2μM purified SH-DNA (red) and 2μM non-purified SH-DNA was shown in **Figure 4-8B.** The refractive angle change of purified SH-DNA was higher than non-purified SH-DNA, 0.25° for purified SH-DNA and 0.21° for non-purified SH-DNA. As shown in **Figure 4-8A**, the time of complementary 100nM DNA loop hybridized with SH-DNA on gold surface was 105 minutes and after 30 minutes washing with HEPES buffer, the signal almost remained the same level which attributes to the tight binding of DNA loop with SH-DNA. Red bar graph in **Figure 4-8B** shows the refractive angle change of 100nM DNA loop in pure system was 0.19° while the refractive angle change of 100nM DNA loop in non-purified system was 0.13°. **Figure 4-8A** shows the time of 150nM MB-DNA hybridized with 2μM SH-DNA and 100nM DNA loop was 110 minutes. Also after 30 minutes washing with HEPES buffer, the refractive angle of MB-DNA stability was same as that before washing, showing that MB-DNA had tight binding with SH-DNA and DNA loop. The blue bar graph was shown in **Figure 4-8B**, the refractive angle change of MB-DNA in pure system is 0.1° while the refractive angle change of MB-DNA in non-purified system was 0.072°. The sensitivity of MB-DNA increased 39% comparison with non-purified/purified SH-DNA based DNA loop structure. It provides further evidence that free thiols competed immobilization on gold surface with SH-DNA and thus dramatically influence sensitivity of DNA loop based ECPA system.

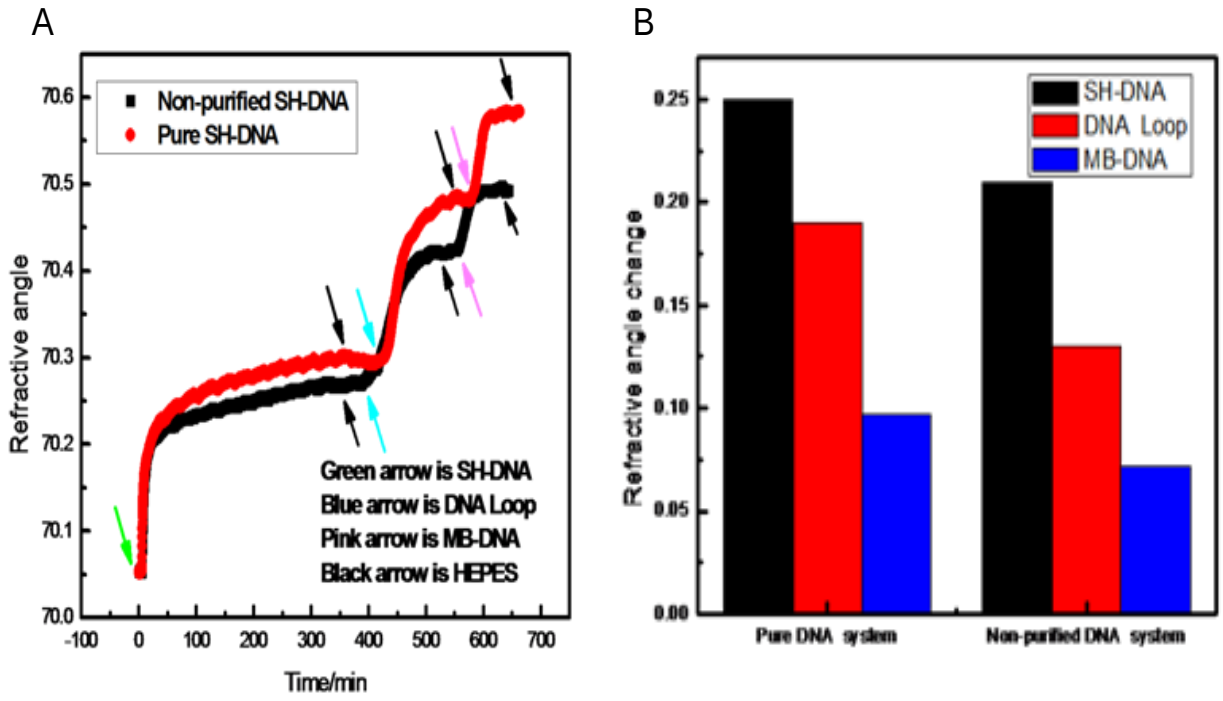

Figure 4-8: Analysis of sensitivity of purified/ non-purified SH-DNA based DNA Loop structure. (A) Sensogram of purified/ non-purified SH-DNA based DNA Loop system. (B) Bar graph of refractive angle change in SH-DNA (black), DNA loop (red), MB-DNA (blue) in non-purified/ purified SH-DNA based DNA Loop structure.

4.6 Effect of free thiols to pure SH-DNA ratio in SPR measurement

As shown in **Figure 4.9**, by monitoring the changes in the percentages of the MCH to purified SH-DNA we observed the effect of impurities present in the TCEP treated oligomers on the assembly and sensitivity of the resulting films. When relatively pure MCH was used the refractive angle change as observed by SPR was lower as the surface coverage with time increases. The sensogram reached stable at ΔRf=0.14 corresponding to 100% MCH. In contrast highest refractive angle change of 0.25° was observed for 100% purified SH-DNA. As the percentages of purified DNA increased by 25% (as shown by cartoons) the signal tend to show the increase in refractive and found to be 0.14°, 0.19°, 0.215°, 0.223°, 0.25°. This coincides with previous reports that after the

initial SH-ss DNA adsorption, the free thiols and other reductant sulphur derivatives incorporated into these films as non DNA contaminants as surface coverage increases with time. This also led to saturation of the SPR signal very early and the presence of nonspecifically bound thiols may explain the lower signals obtained in the formation of ECPA system.

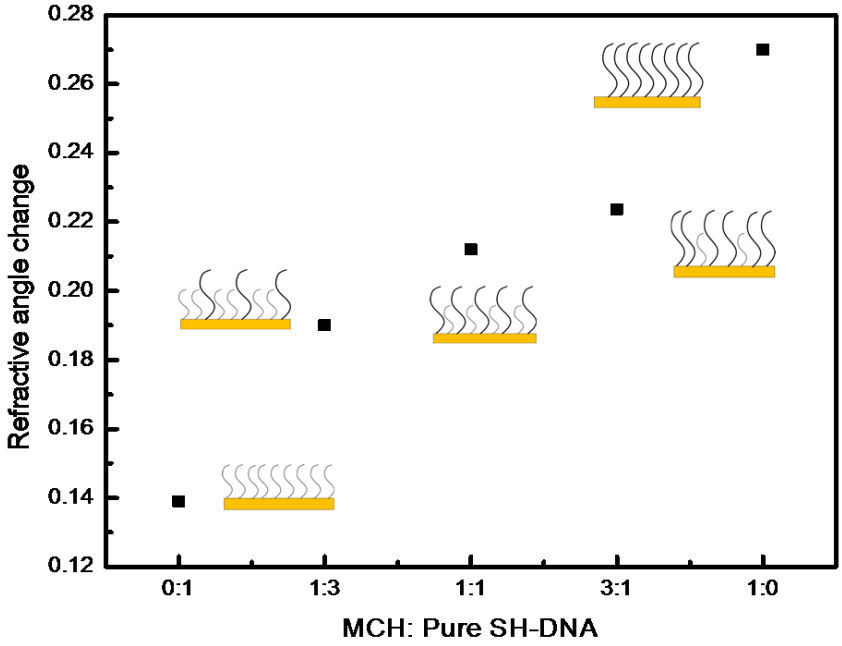

Figure 4-9: Analysis of ratio effect of SH-DNA and free thiols (MCH). Five ratio shown in figure: 100% MCH, 75%MCH and 25% SH-DNA, 50% MCH and 50% SH-DNA, 25% MCH and 75% SH-DNA

Chapter 5: Conclusion and Perspective

5.1 Conclusion

A surface plasmon resonance based sensing system for continuous monitoring of DNA Loop based ECPA on gold surface has been developed. DNA loop oligonucleotides and MB-DNA sequences were alternatively hybridized with SH-DNA sequence for immobilization on gold surface. Surface plasmon resonance demonstrated obvious increase on refractive angle change to monitor SH-DNA immobilization and hybridization with DNA loop and MB-DNA. In elimination of counterpart of SH-DNA or DNA loop, the sensogram had shown no obvious refractive angle change, presenting the incompletion in DNA loop-like structure. Moreover, with filtration matrix, the signal enhancement of SH-DNA immobilization on gold surface was achieved, demonstrating the effect of free thiols. Furthermore, analysis of purified SH-DNA based DNA loop system and non-purified SH-DNA based DNA loop system, confirmed that the presence of free thiols which can compete on gold surface with SH-DNA and thus affect sensitivity of whole system. To study the effect of contaminator of free thiols, mixture of different percentages of SH-DNA and free thiols stated clearly that high percentage of SH-DNA and low percentage of free thiols contribute to increment of refractive angle change. It demonstrated the effect of free thiols have competence on gold surface. With this proof of concept study of dynamics of DNA loop system, this study improves the speed and the sensitivity of ECPA based biosensor system.

5.2 Future work

5.2.1 Evaluation of MB label

For electrochemical detection, in the presence of the target protein, the five part complex move the redox-active MB conjugated with a DNA sequence close to gold surface for transferring the electrons and thus the current signal is proportional to the amount of target protein. However for the SPR experiments, the surface mass is correlated with the refractive index change, so it is not necessary to use the MB labeling. Therefore, our future direction will be to investigate on the comparison of MB labeled and unlabeled DNA using ECPA model system under fixed concentrations of other complementary DNA sequences.

5.2.2 Evaluation of feasibility of real-time protein detection

Currently, DNA loop is used as a model for the antibody based insulin or aptamer based thrombin ECPA system. This DNA loop based model can be made cost effective upon optimization of time and conditions required for thiolated DNA binding. Conditions such as increasing concentrations of protein, flow rate will be investigated.

Reference

1. Dictionary, M.-W., *sensor*. 2015, Merriam-Webster, Incorporated.
2. Janata, J., *Principles of Chemical Sensors*. 2010, Springer Science & Business Media.
3. Eggins, B.R., *Chemial sensors and biosensors. Analytical techniques in the sciences*. 2002, Hoboken, NJ: Wiley.
4. Sang, S., W. Zhang, and Y. Zhao, *Review on the Design Art of Biosensors*. State of the Art in Biosensors - General Aspects. 2013.
5. Cagnin, S., et al., *Overview of Electrochemical DNA Biosensors: New Approaches to Detect the Expression of Life.* Sensors, 2009. **9**(4): p. 3122-3148.
6. Craig, F. *How DNA Works*. 2007; Available from: http://science.howstuffworks.com/life/cellular-microscopic/dna.htm.
7. Watson, J.D. and F.H. Crick, *Molecular structure of nucleic acids.* Nature, 1953. **171**(4356): p. 737-738.
8. Palek, E. and M. Fojta, *Peer reviewed: detecting DNA hybridization and damage.* Analytical Chemistry, 2001. **73**(3): p. 74 A-83 A.
9. Drummond, T.G., M.G. Hill, and J.K. Barton, *Electrochemical DNA sensors.* Nature biotechnology, 2003. **21**(10): p. 1192-1199.
10. Park, J.-Y. and S.-M. Park, *DNA hybridization sensors based on electrochemical impedance spectroscopy as a detection tool.* Sensors, 2009. **9**(12): p. 9513-9532.

11. Hashimoto, K., K. Ito, and Y. Ishimori, *Novel DNA sensor for electrochemical gene detection.* Analytica Chimica Acta, 1994. **286**(2): p. 219-224.

12. Heller, A., *Amperometric biosensors.* Current opinion in biotechnology, 1996. **7**(1): p. 50-54.

13. Bratov, A., N. Abramova, and A. Ipatov, *Recent trends in potentiometric sensor arrays—A review.* Analytica chimica acta, 2010. **678**(2): p. 149-159.

14. Balasubramanian, S.G.S., *Development of smart functional surfaces for biosensor applications*. 2008: ProQuest.

15. Dahmen, E.A.M.F., *Electroanalysis: Theory and Applications in Aqueous and Non-Aqueous Media and in Automated Chemical Control* 1986 Elsevier.

16. Yoon, J.-Y., *Introduction to Biosensors.* 2013.

17. Bunde, R.L., E.J. Jarvi, and J.J. Rosentreter, *Piezoelectric quartz crystal biosensors.* Talanta, 1998. **46**(6): p. 1223-1236.

18. Lu, C. and A.W. Czanderna, *Applications of piezoelectric quartz crystal microbalances*. 2012: Elsevier.

19. Gautschi, G., *Piezoelectric sensorics: force, strain, pressure, acceleration and acoustic emission sensors, materials and amplifiers*. 2002: Springer Science & Business Media.

20. Fan, X., et al., *Sensitive optical biosensors for unlabeled targets: A review.* analytica chimica acta, 2008. **620**(1): p. 8-26.

21. Brecht, A. and G. Gauglitz, *Recent developments in optical transducers for chemical or biochemical applications.* Sensors and Actuators B: Chemical, 1997. **38**(1): p. 1-7.

22. David L. Nelson, A.L.L., Michael M. Cox, *Lehninger Principles of Biochemistry*. 2008, Macmillan.

23. Griffiths, P.R. and J.A. De Haseth, *Fourier transform infrared spectrometry*. Vol. 171. 2007: John Wiley & Sons.

24. Weckhuysen, B.M., *Ultraviolet-visible spectroscopy*. 2004, American Scientific Publishers: Stevenson Ranch, CA. p. 255-270.

25. Lakowicz, J.R., *Principles of fluorescence spectroscopy*. 2007: Springer Science & Business Media.

26. Hendrik Christoffel Hulst, H.C.v.d.H., *Light Scattering by Small Particles*. 1957, Courier Corporation.

27. Baldini, F., *Optical Chemical Sensors*. 2006, Springer Science & Business Media.

28. Janata, J.í., *Optical Sensors*, in *Principles of Chemical Sensors*. 2009, Springer. p. 267-311.

29. Zappe, H., *Fundamentals of Micro-Optics* 2010, Cambridge University Press.

30. Wood, R.W., *XLII. On a remarkable case of uneven distribution of light in a diffraction grating spectrum.* Philosophical Magazine Series 6, 1902. **4**(21): p. 396-402.

31. Rayleigh, L., *On the Dynamical Theory of Gratings.* Proceedings of the Royal Society of London. Series A, Containing Papers of a Mathematical and Physical Character, 1907. **79**(532): p. 399-416.

32. Fano, U., *The Theory of Anomalous Diffraction Gratings and of Quasi-Stationary Waves on Metallic Surfaces (Sommerfeld’s Waves).* Journal of the Optical Society of America, 1941. **31**(3): p. 213-222.

33. Ritchie, R.H., *Plasma Losses by Fast Electrons in Thin Films.* Physical Review, 1957. **106**(5): p. 874-881.

34. Powell, C.J. and J.B. Swan, *Origin of the Characteristic Electron Energy Losses in Aluminum.* Physical Review, 1959. **115**(4): p. 869-875.

35. Kretschmann, E. and H. Raether, *Radiative decay of non radiative surface plasmons excited by light(Surface plasma waves excitation by light and decay into photons applied to nonradiative modes).* Zeitschrift Fuer Naturforschung, Teil A, 1968. **23**: p. 2135.

36. Otto, A., *Excitation of nonradiative surface plasma waves in silver by the method of frustrated total reflection.* Zeitschrift für Physik, 1968. **216**(4): p. 398-410.

37. Liedberg, B., C. Nylander, and I. Lunström, *Surface plasmon resonance for gas detection and biosensing.* Sensors and actuators, 1983. **4**: p. 299-304.

38. Tudos, A.J. and R.B. Schasfoort, *Introduction to surface plasmon resonance.* Handbook of surface Plasmon resonance, 2008: p. 1-14.

39. Homola, J., S.S. Yee, and G. Gauglitz, *Surface plasmon resonance sensors: review.* Sensors and Actuators B: Chemical, 1999. **54**(1): p. 3-15.

40. Pattnaik, P., *Surface plasmon resonance.* Applied biochemistry and biotechnology, 2005. **126**(2): p. 79-92.

41. Karabchevsky, A., S. Karabchevsky, and I. Abdulhalim, *Nanoprecision algorithm for surface plasmon resonance determination from images with low contrast for improved sensor resolution.* Journal of Nanophotonics, 2011. **5**(1): p. 051813-051813-12.

42. Homola, J., *Surface plasmon resonance sensors for detection of chemical and biological species.* Chemical reviews, 2008. **108**(2): p. 462-493.

43. Jönsson, U., et al., *Real-time biospecific interaction analysis using surface plasmon resonance and a sensor chip technology.* Biotechniques, 1991. **11**(5): p. 620-627.

44. Homola, J., *Surface Plasmon Resonance Based Sensors*. 2006, Springer Science & Business Media.

45. Wang, X. and S. Uchiyama, *Polymers for Biosensors Construction*. State of the Art in Biosensors - General Aspects. 2013.

46. Lee, C.-Y., et al., *Evidence of Impurities in Thiolated Single-Stranded DNA Oligomers and Their Effect on DNA Self-Assembly on Gold.* Langmuir, 2005. **21**(11): p. 5134-5141.

47. Lim, H., et al., *Heterobifunctional modification of DNA for conjugation to solid surfaces.* Analytical and Bioanalytical Chemistry, 2010. **397**(5): p. 1861-1872.

48. Lee, C.-Y., et al., *Surface Coverage and Structure of Mixed DNA/Alkylthiol Monolayers on Gold: Characterization by XPS, NEXAFS, and Fluorescence Intensity Measurements.* Analytical Chemistry, 2006. **78**(10): p. 3316-3325.